Published in final edited form as:
J Comp Neurol. 2014 October 15; 522(15): 3539–3554. doi:10.1002/cne.23623.

Local and Commissural IC Neurons Make Axosomatic Inputs on Large GABAergic Tectothalamic Neurons

Tetsufumi Ito[1,2] and **Douglas L. Oliver**[3]

[1]Department of Anatomy, Faculty of Medical Sciences, University of Fukui, Eiheiji, Fukui, 910-1193, Japan

[2]Research and Education Program for Life Science, University of Fukui, Fukui, Fukui, 910-8507, Japan

[3]Department of Neuroscience, University of Connecticut Health Center, Farmington, CT, 06030-3401

Abstract

Large GABAergic (LG) neurons are a distinct type of neuron in the inferior colliculus (IC) identified by their dense VGLUT2-containing axosomatic synaptic terminals. Yet, the sources of these terminals are unknown. Since IC glutamatergic neurons express VGLUT2, and IC neurons are known to have local collaterals, we tested the hypothesis that these excitatory, glutamatergic axosomatic inputs on LG neurons come from local axonal collaterals and commissural IC neurons. We injected a recombinant viral tracer into the IC which enabled Golgi-like GFP labeling in both dendrites and axons. In all cases, we found terminals positive for both GFP and VGLUT2 (GFP+/VGLUT2+) that made axosomatic contacts on LG neurons. One to six axosomatic contacts were made on a single LG cell body by a single axonal branch. The GFP-labeled neurons giving rise to the VGLUT2+ terminals on LG neurons were close by. The density of GFP+/VGLUT2+ terminals on the LG neurons was related to the number of nearby GFP-labeled cells. On the contralateral side, a smaller number of LG neurons received axosomatic contacts from GFP+/VGLUT2+ terminals. In cases with a single GFP-labeled glutamatergic neuron, the labeled axonal plexus was flat, oriented in parallel to the fibrodendritic laminae, and contacted 9–30 LG cell bodies within the plexus. Our data demonstrated that within the IC microcircuitry, there is a convergence of inputs from local IC excitatory neurons on LG cell bodies. This suggests that LG neurons are heavily influenced by the activity of the nearby laminar glutamatergic neurons in the IC.

Keywords

inferior colliculus; vesicular glutamate transporter; GABA; auditory system; excitatory axosomatic synapse; RRID: AB_2278725; RGD ID: 1566430

Corresponding Author: Tetsufumi Ito, Department of Anatomy, Faculty of Medical Sciences, University of Fukui, Eiheiji, Fukui, 910-1193, Japan, Telephone number: +81-776-61-8302, itot@u-fukui.ac.jp.

Conflict of interest:
The authors declare no conflict of interest.

Author contributions:
Study concept and design: TI and DLO. Acquisition of data: TI. Analysis and interpretation of data: TI and DLO. Drafting of the manuscript: TI and DLO. Statistical analysis: TI.

Introduction

The inferior colliculus (IC) is a key midbrain center of the auditory system that receives inputs from virtually all lower auditory brainstem nuclei. In addition to the ascending inputs, most IC neurons emit local axon collaterals (Oliver et al., 1991; Wallace et al., 2012). Thus, there is a complex convergence of local and ascending inputs on neurons in the IC that creates a complex internal microcircuitry. Recent physiological studies have emphasized the importance of the local connections within the IC for the neural processing of sound (Chandrasekaran et al., 2013; Grimsley et al., 2013; Sivaramakrishnan et al., 2013). Nevertheless, little is known about how specific neuron types in the IC contribute to the local microcircuitry.

In the IC, large GABAergic (LG) neurons are tectothalamic neurons with dense axosomatic excitatory inputs from presynaptic terminals that contain the vesicular glutamate transporter 2 (VGLUT2) (Geis and Borst, 2013; Ito et al., 2009; Ito and Oliver, 2012a). Previously, we used retrograde labeling and VGLUT gene expression to identify possible sources of the dense VGLUT2 axosomatic terminals. The IC received inputs from neurons with VGLUT2 message in the dorsal cochlear nucleus, superior olivary complex, and intermediate nucleus of the lateral lemniscus. IC neurons with VGLUT2 expression were also labeled (Ito and Oliver, 2010). Therefore, there are both local and ascending VGLUT2 inputs to the IC, yet it is not known to what extent these inputs synapse on the LG neurons.

In this study, we asked whether local and commissural IC excitatory neurons make VGLUT2 axosomatic inputs on LG neurons. We used a recombinant viral vector that promotes green fluorescent protein (GFP)-labeling of dendrites and axons in Golgi-like manner. VGLUT2+ terminals from local IC neurons were found to make axosomatic inputs on LG neurons. The results demonstrated that LG neurons receive converging inputs from multiple local excitatory neurons, and this suggests a pivotal role in integrating sound information within the IC microcircuitry.

Materials and methods

Subjects and viral injections

Seventeen Long-Evans rats (RGD ID: 1566430) of both sexes were used in this study (Table 1). All experiments were conducted in accordance with institutional guidelines at the University of Fukui and the University of Connecticut Health Center. All efforts were made to minimize the number of animals used and their suffering.

Rats were anesthetized with ketamine (97.6 mg/kg, i.m.) and xylazine (2.4 mg/kg, i.m.). After animals were positioned in a stereotaxic apparatus, a craniotomy was made in the parietal bone, and a glass micropipette filled with palGFP Sindbis viral solutions (Furuta et al., 2001) was advanced into the IC. The viral solution (0.1–1.0 μl) was pressure-injected using nitrogen gas and a custom-made device.

After a survival period of 36–48 hours, rats were re-anesthetized with ketamine and xylazine and perfused transcardially with 4% paraformaldehyde in 0.1 M phosphate buffer (PB; pH

7.4, room temperature). In cases 13-11 and 13-12, animals were perfused with 4% paraformaldehyde and 0.05% glutaraldehyde in 0.1 M PB instead. After cryoprotection with 30% sucrose in PB at 4 °C for 1–2 days, 40 μm-thick serial coronal sections of the brainstem were cut with a freezing microtome from the rostral medial geniculate body to a point caudal to the dorsal cochlear nucleus. Every 6th section was temporarily mounted on non-coated glass slides, cover-slipped with 0.05 M phosphate-buffered saline (PBS), and examined under a fluorescent microscope (BX-51, Olympus Corporation, Tokyo, Japan) to confirm the injection site and to make a rough estimate of the number of infected neurons. After the examination, the sections were floated off gently from the glass slides with a wet brush, and stored in PBS containing 2% sodium azide at 4 °C together with other non-examined sections.

In this study, we chose viral tracers over conventional anterograde tracers since neurons infected with the viral tracer make a fluorescent protein in their cell bodies and there is no background labeling outside of the infected neurons. Consequently, the labeled neurons and processes are easily visualized and can be studied with compatible multi-channel immunofluorescent labeling methods. We discarded any case where axons of passage were labeled and the cell bodies from those axons were visualized outside the IC. Such cases were rare and are not included in Table 1.

Antibodies

In this study, a mouse monoclonal antibody was used for glutamic acid decarboxylase 67 (GAD67; antiserum MAB5406, Millipore, Billerica, MA, RRID: AB_2278725); rabbit polyclonal antibodies were used for VGLUT2 (Fujiyama et al., 2001) and GFP (Tamamaki et al., 2000); and a guinea pig polyclonal antibody was used for VGLUT2 (Fujiyama et al., 2001) (Table 2). GFP and VGLUT2 antibodies were gifts from Professor Takeshi Kaneko (Kyoto University).

The immunogen used for anti-GAD67 antibody was recombinant whole protein of rat GAD67. In the previous study (Ito et al., 2007), we confirmed the specificity of the anti-GAD67 by western blot and preabsorption test. In the western blot, a single band around 67kDa was detected (which is also described in manufacturer's sheet). No signal was detected in rat brain sections incubated with the antibody (1:3000) preabsorped with recombinant rat GAD67 protein (180 μg/ml). Furthermore, staining pattern of the antibody was highly consistent with a previous atlas study (Mugnaini and Oertel, 1985).

The immunogen used for anti-VGLUT2 antibody was synthetic peptide to C-terminal amino acid residues CWPNGWEKKEEFVQESAQDAYSYKDRDDYS of rat VGLUT2 (aa. 554–582). Specificity for the antibody was characterized by western blot and absorption test (Fujiyama et al., 2001). In the western blot, a single band around 62kDa was detected. No signal was detected in rat brain sections incubated with antibody preabsorped with 10000-fold (in mol) excess amount of the synthetic peptide used for the immunization.

The immunogen used for anti-GFP antibody was recombinant whole protein of enhanced green fluorescent protein. The specificity of GFP antibody was confirmed by the absence of staining in rat brain which did not receive viral injections.

Non-fluorescent immunohistochemistry

In 14 cases, an injection of palGFP Sindbis virus resulted in a moderate to heavy infection, and GFP-labeling of cells was found in the IC. In those cases, every sixth section was incubated overnight with rabbit anti-GFP (0.2 μg/ml) diluted in incubation buffer (1% normal donkey serum, 0.3% Triton X-100, 0.2% sodium azide, and PBS). The next day, sections were washed and incubated for an hour with donkey biotinylated anti-rabbit IgG (1:200; Jackson Immunoresearch, West Grove, PA) followed by an incubation for 1 hour with avidin-biotinylated horseradish peroxidase complex (1:50; ABC Elite, Vector Laboratories, Burlingame, CA). Bound peroxidase was visualized as a dark blue stain with a nickel-diaminobenzidine reaction. The sections were mounted on coated glass slides, counterstained with Neutral Red (Merck, Whitehouse Station, NJ), dehydrated, cleared with xylene, and cover-slipped with Entellan (Merck).

Immunofluorescent labeling

In 14 cases that showed multiple cell labeling, every sixth section was incubated overnight with mouse anti-GAD67 (1:1000), guinea pig anti-VGLUT2 (0.5 μg/ml), and rabbit anti-GFP (0.5 μg/ml) diluted in incubation buffer. The next day, sections were washed and incubated for 3 hours with donkey AlexaFluor488-conjugated anti-rabbit IgG (1:200; Life Technologies), Cy3-conjugated anti-guinea pig IgG, and Cy5-conjugated anti-mouse IgG (1:200; Jackson). Sections were mounted on coated glass slides, air dried, rehydrated, and cover-slipped with 1,4-diazabicyclo[2.2.2]octane (DABCO).

Combination of fluorescent immunohistochemistry and immunoelectron microscopy

In cases 13-11 and 13-12, the sections were first examined by fluorescent immunohistochemistry, and then examined by immunoelectron microscopy in the following manner: First, every sixth section was incubated overnight with mouse anti-GAD67, rabbit anti-GFP, and guinea-pig anti-VGLUT2 diluted in incubation buffer which does not contain Triton X-100. The following day, sections were washed and incubated overnight with donkey Cy3-conjugated anti-guinea pig IgG, Cy5-conjugated anti-mouse IgG, and AlexaFluor488-conjugated anti-rabbit IgG. The sections were mounted on glass slides and cover-slipped with DABCO, and imaged with a confocal laser scanning microscope (CLSM, Leica TCS SP3, Leica Microsystems, Wetzlar, Germany). After imaging, the sections were washed with PBS, incubated overnight with rabbit anti-GFP, then incubated overnight with donkey biotinylated anti-rabbit IgG, and incubated 3 hours with ABC-Elite. Bound peroxidase was visualized with a diaminobenzidine reaction. Then the sections were postfixed for 30 min with 1% osmium tetraoxide diluted in PB, *en bloc* stained with uranyl acetate overnight, dehydrated with graded ethanol, substituted with propylene oxide, and embedded in Epok812 (Oken Shoji, Japan). Serial ultrathin sections were made with an ultramicrotome (EM FCS, Leica Microsystems, Germany) and observed with an electron microscope (H7650, Hitachi, Japan).

Combination of fluorescent and bright field immunohistochemistry

In 3 cases that had single cell labeling with GFP (10-95, 11-13, 11-14; Table 1), the phenotype of the neurotransmitters was examined by fluorescent immunohistochemistry,

then the labeled neuron was visualized by chromophoric immunohistochemistry together with GABAergic cells in the following manner: First, a complete series of sections was incubated overnight with mouse anti-GAD67, rabbit anti-GFP, and guinea-pig anti-VGLUT2 diluted in incubation buffer. The following day, sections were washed and incubated for 3 hours with donkey Cy3-conjugated anti-guinea pig IgG, Cy5-conjugated anti-mouse IgG, and biotinylated anti-rabbit IgG. Sections were mounted on glass slides and cover-slipped with DABCO. Colocalization of GFP and the other markers in cell bodies and terminals were examined with a CLSM. After imaging, the sections were washed with PBS together with other sections, incubated for 1 hour with mouse anti-GAD67, and then incubated for 1 hour with donkey alkaline phosphatase-conjugated anti-mouse IgG (1:500; Jackson) and ABC-Elite. Bound peroxidase was reacted for 30 minutes with biotinylated tyramide (TSA-biotin, Perkin-Elmer, Waltham, MA) to amplify GFP+ signal. Sections were incubated again for an hour with ABC-Elite. Then, the bound peroxidase was made visible as brownish stain with a diaminobenzidine reaction. Sections were washed briefly with TS9.5 solution, consisting of 0.1 M Tris-HCl (pH 9.5), 0.15 M sodium chloride, and 10 mM magnesium chloride. Bound alkaline phosphatase was visualized as navy blue stain in the presence of nitro blue tetrazolium chloride/ 5-bromo-4-chloro-3-indolyl phosphate toluidine salt NBT/BCIP; (Roche) in 0.05% levamizole (Vector)/ 0.1% Tween 20/ TS9.5 for 30 minutes. Finally, the sections were mounted on coated glass slides, dehydrated, cleared with xylene, and cover-slipped with Entellan. Photomicrographs were taken with a digital camera (QICAM, QImaging, Surrey, Canada).

Imaging of fluorescent materials

Fluorescent micrographs were acquired with a CLSM. GFP and AlexaFluor488 were excited by a 488 nm Ar laser, and emitted fluorescence was filtered with a 500–530 nm band-pass filter. Cy3 was excited by a 543 nm He-Ne laser, and emitted fluorescence was filtered with a 565–615 nm band-pass filter. Cy5 was excited by a 633 nm He-Ne laser, and emitted fluorescence was filtered with a 650 nm low-pass filter. Z-stack images of each dye were taken sequentially to avoid bleed-through artifact. The image stacks were deconvoluted to remove out-of-focus signals with Huygens Essential software (Scientific Volume Imaging, Hilversum, Netherlands). Minimal adjustments of the fluorescent intensity levels were made on the deconvoluted images in Photoshop CS3 (Adobe Systems, San Jose, CA).

Single cell reconstruction

In the single cell labeling cases (10-95, 11-13, and 11-14), GFP+ cell bodies, dendrites, dendritic spines, and axons were reconstructed from serial sections with Neurolucida software (MBF Bioscience, Williston, VT). In addition, GAD67+ cell bodies which receive axosomatic contacts from GFP+ axons were plotted with Neurolucida. We used the Neurolucida traces to analyze the total length of axons and dendrites, density of spines, and spatial distribution of the GAD67+ cell bodies with axosomatic contacts. To determine whether the GAD67+ cells with axosomatic contacts were scattered on the same plane, coordinates of the GAD67+ cells were further analyzed by principal component analysis with MATLAB Statistics Toolbox (version: R14; Mathworks, Natick, MA). The principal component analysis was used to fit a plane to the XYZ coordinates of the GAD67+ cells receiving contacts. The 1st principal component is the eigenvector that accounts for the

largest variance, the 2nd principal component is the vector that accounts for the second largest variance and is perpendicular to the 1st principal component. A plane parallel to both the 1st and 2nd principal components was calculated as the planar fit of the GAD67+ cells. Therefore, the standard deviation (SD) of the 3rd principal component score indicates the fit of the GAD67+ cell bodies to the plane. To visualize the fit of axons, dendrites, and GAD67+ cell bodies, traces were rotated on the medio-lateral axis since IC laminae are not perpendicular to coronal sectional plane. To obtain the rotation angle, we calculated an angle between the rostro-caudal axis and the intersection of the planar fit and the sagittal plane. The tracing was rotated with Neurolucida Explorer software.

Terminal analysis of single cell labeling cases

To analyze termination pattern of a single IC axon on GAD67+ cells, GAD67+ cell bodies that received axosomatic contacts from GFP+ axons were examined with ×40 dry lens (NA = 0.95) and ×100 oil-immersion lens (NA = 1.4), and traced along with neighboring GFP+ axons with the aid of a camera lucida. Then, the camera lucida drawings of GAD67+ neurons and GFP+ axons were further examined. If an axon branch terminated on a GAD67+ cell body, the axon swellings on the cell body were defined as “terminal boutons”. If an axon branch passed by a GAD67+ cell body and the axon’s swellings made contact on the cell body, the swellings were defined as “*en passant* varicosities”. The number of contact of both categories was counted for each axon branch. If a GAD67+ cell was innervated by several axonal branches, the number of the axon branches was counted.

Terminal analysis for fluorescent images

Images of LG neurons were acquired with a CLSM with a ×63 oil-immersion lens (NA = 1.4). For imaging terminal contacts on cell bodies, we took Z-stacks images at ×32 optical zoom, which is maximal magnification of the system, at a z-interval of 113 nm. Deconvoluted fluorescent image stacks were analyzed and visualized with custom-made software written in MATLAB. Z-stack high-magnification images of LG cells and their surrounding structures were analyzed for the termination of a single axon. Z-stacks obtained inside the injection site were not used for analysis since it was not possible to isolate single axons in such Z-stacks. The remaining Z-stacks contained 1–5 axons. Three-dimensional reconstructions of single axons and cell bodies of LG cells were made from the Z-stacks, and the volume of GFP+ terminals and the surface area of LG cell bodies were calculated from the reconstructions.

Spatial distribution of cell bodies of LG and GFP+ neurons

To analyze the spatial distribution of LG cells that received axosomatic contact with terminals positive for both GFP and VGLUT2, a series of every 6th section was re-scanned in 4 rats (10-04, 10-10, 13-11, and 13-12). First, images covering the whole IC were acquired with a ×20 objective lens, and low-magnification montages of IC sections were made. Next, the IC was examined with a fluorescent microscope attached to a CLSM. If GFP+ terminals were found in the field of view, Z-stack images from the top to bottom of the section were taken with the CLSM with a ×40 oil-immersion lens (NA = 1.25) at a voxel size of 0.366 × 0.366 × 1 μm. The maximal projection of the Z-stack images were

superimposed on the low-magnification montages, and if LG cell bodies receiving axosomatic contact with terminals positive for both GFP and VGLUT2 (GFP+/VGLUT2+) were found, the loci of the cell bodies were plotted on the montages. We were able to distinguish GFP+ neurons from GFP+ glial cells by examining morphology of their processes in Z-stack images. Only cells with clear dendrites were counted as neurons while cells with ambiguous morphology were not counted. Cell bodies of GFP+ neurons were plotted on the montages. The raw montages and the montages with plots of cell bodies of LG and GFP+ neurons were both imported to Neurolucida software. Subdivisions of the IC were drawn from VGLUT2 and GAD67 staining pattern of the montage and neighboring Neutral-red stained sections. Coordinates of cell bodies of LG and GFP+ neurons were exported and further analyzed with MATLAB. All statistical analyses except for principal component analysis were done with R software (version 2.15.2; http://www.r-project.org/) and custom-made scripts.

Results

IC local and commissural axons make excitatory axosomatic contact on LG cells

Large injections of palGFP Sindbis viral solution into the IC resulted in the infection of many neurons and glial cells (Fig. 1A, squares; Tables 1 and 3). Most GFP+ neurons (93%) were not GABAergic since they were negative for GAD67 (Table 3). As a result, GFP colocalized with VGLUT2 in most axonal terminals, while colocalization of GAD67 and GFP was rare.

Local axons from infected IC neurons made axosomatic contacts on LG neurons (Fig. 1A, dots). This labeling pattern is illustrated by a case that received an injection in the IC in the ventrolateral central nucleus and the adjacent lateral cortex (ICC and ICL; case 10-04; Fig. 1A). An example of a LG cell located in the injection site (Fig. 1A, an open arrow) is shown in Fig. 2A. The LG cells were identified by GAD67 immunolabeling in the cell bodies (e.g., Fig. $2A_4$, an asterisk) surrounded by dense VGLUT2+ axosomatic endings (green, Fig. $2A_3$). There were numerous GFP+ fibers (red, Fig. $2A_2$) in the vicinity of the neuron and some of these terminals made contact with the cell bodies or dendrites of the LG cells (Fig. 2A, B). Most GFP+ terminals also contained VGLUT2 (arrows in Fig. 2B). Here and in the following figures, the double labeling is seen in 3 views: A single optical-sectioned image in the original plane of section and two side views of the Z-stack that are shown above and to the right of the image in the normal plane (Fig. $2B_2$–B_3). Both the GFP+ and VGLUT2+ profiles matched in all three views indicating that the 2 molecules were colocalized rather than in different z positions. Thus, some of excitatory axosomatic endings on the LG cells are from local axons.

At more remote locations from the injection site, there were fewer GFP+ axons around LG cells (Fig. 2C). Figure 2C shows a LG cell in the ipsilateral dorsal cortex of the IC (ICD) of case 10-04 (Fig. 1A, a filled arrow). A GFP+ axon innervated the LG cell with one axosomatic terminal bouton that was double-labeled with GFP and VGLUT2 (arrows in Fig. 2D). Each LG cell body received contacts from 1–6 GFP+/VGLUT2+ boutons.

LG cells also received inputs from the contralateral IC (Fig. 1B). For example, Figure 2E–F show a single axon from the contralateral IC that made GFP+/VGLUT2+ axosomatic terminals on a LG neuron. The LG neurons receiving axosomatic contacts from GFP+/VGLUT2+ terminals were sparsely distributed in the contralateral IC, mainly in the ICD and ICC. Each LG cell body received contacts from 1–3 GFP+/VGLUT2+ boutons of a contralateral IC neuron. It was clear that a single GFP-labeled axon gave rise to only a few of the numerous VGLUT2+ axosomatic terminals on the somata in these LG neurons.

To assess the extent to which axosomatic contacts observed with light microscopy made actual synaptic contacts, the same LG neurons that received contacts with GFP+/VGLUT2+ terminals were examined with both the CLSM and the electron microscope in cases 13-11 and 13-12. After images of LG neurons were taken with the CLSM (Fig. 3A), the GFP immunoreactivity was visualized by a diaminobenzidine reaction, serial ultrathin sections were cut through the same LG neurons (Fig. 3B), and the GFP+/VGLUT2+ terminals were identified. Single GFP+ terminals were examined in 7 serial ultrathin sections to determine whether the terminals made a synaptic contact on the adjacent LG cell body. In the 45 re-identified GFP+/VGLUT2+ terminals, all contained numerous clear round synaptic vesicles (Fig. 3C) and made a direct contact (without a glial sheath) on the LG cell body. Asymmetric synaptic contacts were observed in 37 of 45 terminals (82.2%; arrowheads in Fig. 3C). In the remainder, the cell membrane was oblique to the plane of section, and the synaptic densities could not be identified in the sections examined. Thus, most axosomatic terminals identified by light microscopy made synaptic contacts between GFP+/VGLUT2+ terminals and the LG cell bodies.

Proximity of presynaptic excitatory IC neurons to postsynaptic LG neurons

The number of LG neurons receiving axosomatic contacts from GFP+/VGLUT2+ terminals was largest in the subdivision that received the injection, where the infected neurons were most numerous (Fig. 1A; Table 3). For example, if the infected GFP+ neurons were in the ventral ICC, so were the LG cells receiving contacts. Likewise, GFP+ cells in ventral ICL were adjacent to LG cells in ICL. Both the pre- and postsynaptic cells followed the laminar organization of IC in rat, so they were presumably within the same region of the tonotopic map (Malmierca et al., 2008).

These results suggest that IC GFP+ neurons make contacts on nearby LG cells. To test this, we calculated the distance between all combinations of LG neurons in contact with GFP+/VGLUT2+ terminals and the GFP+ neurons on the ipsilateral side. This was compared to the distance between all combinations of randomly distributed points inside the IC and GFP + neurons. In all cases (n = 4), the cumulative histogram of the observed distance (thick lines in Fig. 4) was steeper than that of the random distribution (dotted lines in Fig. 4) and significantly different ($P < 0.001$, two-sample Kolmogorov-Smirnov test). The median of the observed distance was 871, 766, 747, and 735 μm in the cases 10-04, 10-10, 13-11, and 13-12, respectively. Thus, the local excitatory neurons do not make axosomatic contact randomly but are more likely to make contacts on a nearby LG cell.

Laminar arrangement of LG cells innervated by a single IC neuron

In three injections (10-95, 11-13, 11-14; Table 1), only a single neuron was infected in each IC (Fig. 5). The GFP+ cell bodies were negative for GAD67 (e.g., Fig. 5A), and the axon terminals emitted from these cells were positive for VGLUT2 (Fig. 5B). Therefore, these neurons were glutamatergic IC neurons with local axon collaterals. After processing for bright-field immunohistochemistry, the dendritic morphology of the neuron was reconstructed (Fig. 5C–E). Two neurons (cases 10-95 and 11-13) were located in the ICC and had oriented dendrites (Fig. 5C, D). The third neuron (case 11-14) was located in layer 3 of the ICL and had a pyramidal morphology (Fig. 5E) (Malmierca et al., 2011).

GFP+ axons from these single neurons made contact with large GAD67+ cell bodies in the ipsilateral IC that are likely LG neurons (Fig. 6A). Each labeled axon made contact on 9–30 GAD67+ cell bodies (30 cells, 10-95; 21 cells, 11-13; and 9 cells, 11-14; Table 4; dots in Fig. 6B–D). The GAD67+ cells that received contacts had a mean diameter of 22.3 μm ± 5.54 (mean ± SD, 60 cells). We concluded that these GAD67+ cells receiving the contacts were LG cells since GAD67+ cells with a diameter larger than 16.5 μm are exclusively LG cells (Ito et al., 2009).

In these cases, the GFP+ axons had extensive, oriented local collaterals (Fig. 6B–D). The axonal plexuses of neurons 10-95 and 11-13 had a similar length, but neuron 11-14 had a shorter axonal plexus (Table 4). For these three neurons, the mean distance between GFP+ cell body and GAD67+ cells receiving contacts was relatively small (200–500 μm; Table 4). Since many IC neurons have local axon collaterals that are parallel to the fibrodendritic laminae (Oliver et al., 1991; Wallace et al., 2012), we examined whether or not LG cells receiving contacts from the same IC neuron were distributed in the same plane. If LG cells receiving contacts were distributed in a flat plane, the SD of the 3rd principal component score will approach zero. On the other hand, if the LG cells are distributed randomly, difference between the SD of 3rd principal component score to those of the other principal component scores will be small. Therefore, the SD of the 3rd principal component score can be used to indicate the fit of LG cell distribution to a plane. In cells 10-95 and 11-14, the SDs of the 3rd principal component scores were much smaller than those of the 1st and 2nd principal component scores (Table 5) and resulted in excellent planar fits (Fig. 7A, D). After the traces were rotated along the medio-lateral axis, the presumed postsynaptic LG cells and the axons were well-aligned (Fig. 6B, D). In these cases, the excitatory neuron might influence the LG cells in the same plane for a distance of ~ 500 μm. The clusters of LG neurons that shared the same local inputs (Figs. 6 and 7) were consistent with the distribution of axosomatic contacts in the large injection cases (Figs. 1A and 4).

Cell 11-13 failed to fit a single plane (Fig. 7B). This poor fit is likely due to multiple axonal plexuses rather than an unoriented plexus. Indeed, the axon was distributed into two planar axonal plexuses within the ICC; the larger one invaded the ICD and was close to the GFP+ cell body; while the other was smaller and located ventral to the GFP+ cell body. The same axon also extended into the ICL where it made a third small planar axonal plexus (Fig. 6C). Most LG cells with axosomatic contacts from GFP+ cell 11-13 were located in the largest plexus (14 of 21 LG cells) that contained the GFP-labeled somata. Only a few LG cells were located in the other axonal nests; three were in the ventral plexus and four were in the ICL

plexus. The LG cells within the largest axonal plexus (14 cells) were aligned well to the planar fit (Fig. 7C; Table 5). Within that plane, the excitatory neuron was able to influence LG cells at a distance of ~ 1000 μm. Thus, despite the multiple plexuses, these data support the notion that IC excitatory neurons mainly influence the LG cells within the same fibrodendritic laminae.

Ratio of postsynaptic LG neurons to presynaptic excitatory neurons

Although we observed axosomatic GFP+/VGLUT2+ inputs on LG neurons in all 17 cases, the number of LG neurons that received GFP+/VGLUT2+ axosomatic inputs varied between cases (Table 3). Cases that had more GFP+ neurons in the ICC (10-04 and 13-12) tended to have more LG neurons that received GFP+/VGLUT2+ axosomatic inputs, while a case with less GFP+ neurons in the ICC (13-11) tended to have fewer LG neurons receiving the inputs (Table 3). Furthermore, in the single labeling cases more GAD67+ cells received axosomatic contact from ICC neurons (10-95 and 11-13) than an ICL neuron (11-14). These data imply that more LG neurons receive axosomatic contacts from an excitatory neuron in the ICC than that in the ICL or ICR.

In large injection cases, ratio of GFP+/GAD67− neurons to postsynaptic LG neurons was 1.4 to 13 (calculated from Table 3) and smaller than those of single injection cases (9–30). This lower ratio may be due to the presence of single LG neurons that received inputs from multiple GFP+ neurons. In large injection cases, numerous GFP+ axons made axosomatic contact on LG cells that were close to the injection site (Fig. 2A), while in the single injection cases only a few (1–3) axonal branches terminated on single LG cell bodies. This strongly suggests LG neurons receive multiple axosomatic excitatory inputs from nearby neurons.

Analysis of axonal terminals on LG cell bodies

To determine the size of the GFP+/VGLUT2+ boutons, we measured their volume in deconvoluted image stacks. The median of volume of single terminals from the IC was 2.36 μm^3. Thus, the single terminals had a mean diameter of 1.65 μm. This put them in the category of large or medium terminals, but not small (Nakamoto et al., 2013).

To examine the numbers of contacts received by LG neurons, we examined axons in both bright-field single-cell-labeling specimens (cases 10-95, 11-13, and 11-14) and immunofluorescent materials. In the single-cell cases, we found that some GFP+ axonal branches made *en passant* boutons on GAD67+ cell bodies (Fig. 8A, purple arrows), while others made terminal boutons (Fig. 8A, red arrows). Terminal branches were the final branch of the axon where no further branching was observed. Terminal branches used both terminal boutons and/or *en passant* varicosities to make axosomatic contacts on LG cells. We examined the entire axon in three cases and found that 44 of 76 terminal branches made terminal boutons and the other 32 made boutons *en passant* on LG cell bodies.

We examined the extent to which single LG neurons received axosomatic contact from GFP + axonal branches. Each GAD67+ cell body received a contact from one to six presynaptic endings from GFP+ axons (median: 2; 60 cells). The majority of the GAD67+ cells (46 of

60) received a contact from only one labeled axonal branch. In 23 of 46 cells, the labeled axonal branch made a single contact, while in the other 23 cells the branch made 2 to 5 contacts. Twelve LG cells had contacts from two labeled axonal branches, and two LG cells receive contacts from three branches that arose from the same GFP+ axon. A similar pattern was seen in fluorescent materials (Fig. 8B, C) where 49 terminal branches were found in 27 Z-stack images of LG neurons obtained from 14 rats. The LG cell bodies received a contact from only one terminal branch in 13 Z-stacks, while the LG cell body received contacts from 2–5 terminal branches in 14 Z-stacks. A single terminal branch made one to six axosomatic contacts (median: 2), consistent with the bright-field result. Thus, individual LG cells receive only small numbers of axosomatic contacts from the same axon. At the same time, a single IC excitatory neuron makes only a few axosomatic terminals on a single LG neuron. This suggests that numerous individual axons from separate presynaptic neurons may contribute to the dense axosomatic terminals surrounding the LG cells' somata.

Discussion

In the present study, we demonstrated that the LG neurons in the IC receive axosomatic excitatory inputs from local and commissural IC neurons. Dozens of LG neurons within a single fibro-dendritic lamina in the IC may receive local inputs from one of the glutamatergic neurons in the same lamina. Since the number of contacts from a single axon represents only a small fraction of the dense axosomatic terminals on a LG neuron, these data suggest that the LG neurons receive converging excitatory inputs from dozens of local neurons. These data suggest that the fibro-dendritic lamina contains a microcircuit composed of excitatory neurons activating multiple LG neurons that, in turn, drive thalamic inhibition.

Previous studies of local IC microcircuitry

Local axon collaterals from IC neurons have been shown in previous studies with the Golgi method and with intracellular or juxtacellular labeling (Oliver et al., 1991; Oliver and Morest, 1984; Wallace et al., 2012). Our observations of neurons with laminar axonal plexuses are consistent with the previously studies. However, the previous studies did not define the presynaptic or postsynaptic neuron types based on neurotransmitter synthesis or the presence of other molecular markers. In the present study, both the presynaptic and postsynaptic elements were identified, so this data reveals how many GABAergic LG neurons receive axosomatic innervation from the axon of a single excitatory neuron. Individual glutamatergic axons make a small number of synaptic contacts on a large number of LG neurons. The present data suggests that excitatory neurons in the ICC innervate more LG neurons than those in the IC cortex. This is consistent with previous studies that show ICC neurons have highly branched, laminar local axons, whereas neurons in the IC cortex have less branched, nonlaminar local axons (Oliver et al., 1991).

Previous studies also addressed the issue of how the local microcircuitry distributes information from the ICC to the IC cortex. A recent study of the IC in brain slices showed that electrical stimulation of the lateral lemniscus elicited a rapid depolarization in the ICC but a slow depolarization in the ICL (Chandrasekaran et al., 2013). The ICD was less

frequently activated, and when activated the onset of the response was longer than that in the ICC. After $GABA_A$ receptors were blocked, electric stimulation of lemniscal axons produced a slow and strong response in the ICD. One interpretation of those data is that activity in the IC cortices is controlled by microcircuitry in the ICC containing both excitatory and inhibitory neurons and that the LG neurons are candidates to transmit inhibition from ICC to the IC cortices.

Weak commissural innervation of LG neurons

In addition to the local axonal plexus, IC neurons terminate in the opposite IC via the commissure. On both sides of the IC, there are two plexuses connected by the commissure. The medial band is the fibro-dendritic lamina that extends from ICC into the ICD, whereas the lateral band is the lamina in the ICL (Saldana and Merchan, 1992; Saldana and Merchan, 2005). In all cases, the contralateral axonal plexus is less prominent than the ipsilateral one. In the present study, we observed a contralateral axonal plexus in many cases, but the number of LG neurons receiving axosomatic contacts from commissural neurons was small (Fig. 1B; Table 3). This suggests that the commissural projection has less influence on the LG neurons than the ipsilateral excitatory input.

It is known that the activation of commissural fibers exerts both excitatory and inhibitory effects (Smith, 1992). Such inhibition may arise directly from GABAergic commissural neurons (Gonzalez-Hernandez et al., 1996). A reduction of neural activity in the IC due to the injection of kynurenic acid, a glutamate receptor antagonist, can produced either smaller or larger frequency response areas in the contralateral IC (Malmierca et al., 2003). A larger frequency response area can be explained as loss of inhibition, i.e. a loss of GABAergic commissural input, or it may be due to a reduction of commissural excitation due to activity of local GABAergic neurons. Direct commissural projections of GABAergic neurons are a more likely source of commissural inhibition in the IC. Unfortunately, the targets of the presumed commissural GABAergic neurons have yet to be determined.

Functional implications for local circuitry in IC

Axosomatic synapses from multiple sources are ideal for coincidence detection. In the ventral cochlear nucleus, the octopus neuron is an example of this type of synaptic organization. These cells have a low input resistance and require the summation of well-timed small synaptic potentials from many fibers to generate an action potential (Golding et al., 1995; Oertel et al., 2000). The LG neuron may be a similar detector of coincident activation. Since LG cells have the lowest input resistance among IC cell types and appear to have the best temporal precision of neurons in the IC (Geis and Borst, 2013), the activity of many excitatory axosomatic terminals on LG neurons may be ideal for the generation of a short-latency, well-time response.

The fibrodendritic lamina in the ICC may function as a microcircuit. The circuit is defined by a single glutamatergic neuron that innervates multiple LG neurons in the same IC lamina. This pattern is repeated many times over within the same lamina. Consequently, the activity of many excitatory, VGLUT2 neurons within a lamina results in the coincident activation of the LG neurons within the lamina. Activation of many glutamatergic neurons is necessary

since each local axon only contributes a few axosomatic synapses to each LG neuron, and by itself may be insufficient to drive the LG cell. So, many VGLUT2 neurons may be needed to fire a LG cell. This suggests that stimuli that recruit many neurons within the same lamina will be most effective in bringing the LG neurons to the threshold for firing.

Functional implications for tectothalamic processing

Since both LG and excitatory neurons are predominantly tectothalamic cells, the activity by these neurons may result in short latency inhibition in the medial geniculate body as well as excitation. Since LG neurons are the largest cells in the IC (Ito et al., 2009) and have the largest axons in the brachium of the IC (Saint Marie et al., 1997), it is likely that their axons are faster conducting and the inhibition may precede the excitation in vivo as it does in vitro (Peruzzi et al., 1997). Thus, the LG neurons may regulate the amount and timing of excitation at the thalamic level.

The LG neurons may provide an essential input to a subset of medial geniculate neurons that receive both inhibitory and excitatory tectothalamic inputs (Bartlett and Smith, 2002). A recent study (Venkataraman and Bartlett, 2013) showed that electrical stimulation of the brachium of the IC elicited purely inhibitory response in 41% of medial geniculate neurons at postnatal day 27. It is possible that such neurons are driven exclusively by excitatory inputs from the cerebral cortex, and the ascending sensory information from the LG neurons modulates the corticothalamic input. This implies that the influence of the auditory cortex on the medial geniculate neurons may be altered or blocked by types of acoustic stimuli that activate the LG neurons.

Concluding remarks

The findings from our earlier study (Ito and Oliver, 2012b) in combination with the present results suggest that LG neurons in the IC receive excitatory axosomatic inputs from the lower auditory brainstem nuclei as well as local inputs from the IC. Thus, LG neurons may combine auditory information from ascending pathways with activity in the local microcircuitry of the IC.

Acknowledgments

The authors gratefully acknowledge Dr. Takeshi Kaneko (Kyoto University) for his gift of Sindbis virus and antisera for VGLUT2, GFP, and mRFP, and his critical reading, Drs. Munenori Ono (University of Connecticut Health Center), Nobuaki Tamamaki (Kumamoto University), and Kouichi Nakamura (Oxford University) for their critical reading, Dr. Duck O. Kim (University of Connecticut Health Center) for his donation of equipment, Mr. Hitoshi Takagi (Life Science Research Laboratory, University of Fukui) for his excellent technical assistance for electron microscopy, Dr. Satoshi Iino (University of Fukui) for other support. This work was supported by grants from Ministry of Education, Science and Culture of Japan (Grant number: 22700365 and 25430034, TI), the Uehara Memorial Foundation (TI), the Ichiro Kanehara Foundation (TI), Research and Education Program for Life Science of University of Fukui (TI), and NIH R01 DC00189 (DLO).

Abbreviation list

IC	inferior colliculus
LG	large GABAergic

VGLUT	vesicular glutamate transporter
PB	phosphate buffer
PBS	phosphate-buffered saline
+	positive
DABCO	1,4-diazabicyclo[2.2.2]octane
CLSM	confocal laser-scanning microscope
SD	standard deviation
ICC	central nucleus of the inferior colliculus
ICL	lateral cortex of the inferior colliculus
ICD	dorsal cortex of the inferior colliculus
ICR	rostral cortex of the inferior colliculus
BIC	brachium of the inferior colliculus
PC	principal component
GFP	green fluorescent protein
GAD67	glutamic acid decarboxylase

Literatures cited

Bartlett EL, Smith PH. Effects of paired-pulse and repetitive stimulation on neurons in the rat medial geniculate body. Neuroscience. 2002; 113(4):957–974. [PubMed: 12182900]

Chandrasekaran L, Xiao Y, Sivaramakrishnan S. Functional architecture of the inferior colliculus revealed with voltage-sensitive dyes. Front Neural Circuits. 2013; 7:41. [PubMed: 23518906]

Fujiyama F, Furuta T, Kaneko T. Immunocytochemical localization of candidates for vesicular glutamate transporters in the rat cerebral cortex. J Comp Neurol. 2001; 435(3):379–387. [PubMed: 11406819]

Furuta T, Tomioka R, Taki K, Nakamura K, Tamamaki N, Kaneko T. In vivo transduction of central neurons using recombinant Sindbis virus: Golgi-like labeling of dendrites and axons with membrane-targeted fluorescent proteins. J Histochem Cytochem. 2001; 49(12):1497–1508. [PubMed: 11724897]

Geis HR, Borst JG. Large GABAergic neurons form a distinct subclass within the mouse dorsal cortex of the inferior colliculus with respect to intrinsic properties, synaptic inputs, sound responses, and projections. J Comp Neurol. 2013; 521(1):189–202. [PubMed: 22700282]

Golding NL, Robertson D, Oertel D. Recordings from slices indicate that octopus cells of the cochlear nucleus detect coincident firing of auditory nerve fibers with temporal precision. J Neurosci. 1995; 15(4):3138–3153. [PubMed: 7722652]

Gonzalez-Hernandez T, Mantolan-Sarmiento B, Gonzalez-Gonzalez B, Perez-Gonzalez H. Sources of GABAergic input to the inferior colliculus of the rat. J Comp Neurol. 1996; 372(2):309–326. [PubMed: 8863133]

Grimsley CA, Sanchez JT, Sivaramakrishnan S. Midbrain local circuits shape sound intensity codes. Front Neural Circuits. 2013; 7:174. [PubMed: 24198763]

Ito T, Bishop DC, Oliver DL. Two classes of GABAergic neurons in the inferior colliculus. J Neurosci. 2009; 29(44):13860–13869. [PubMed: 19889997]

Ito T, Hioki H, Nakamura K, Tanaka Y, Nakade H, Kaneko T, Iino S, Nojyo Y. Gamma-aminobutyric acid-containing sympathetic preganglionic neurons in rat thoracic spinal cord send their axons to the superior cervical ganglion. J Comp Neurol. 2007; 502(1):113–125. [PubMed: 17335042]

Ito T, Oliver DL. Origins of Glutamatergic Terminals in the Inferior Colliculus Identified by Retrograde Transport and Expression of VGLUT1 and VGLUT2 Genes. Front Neuroanat. 2010; 4:135. [PubMed: 21048892]

Ito T, Oliver DL. The basic circuit of the IC: tectothalamic neurons with different patterns of synaptic organization send different messages to the thalamus. Front Neural Circuits. 2012a; 6:48. [PubMed: 22855671]

Ito T, Oliver DL. Tectothalamic inhibitory neurons in the inferior colliculus receive converged axosomatic excitatory inputs from multiple sources 2012. Neuroscience Meeting. 2012b 367.305/GG312.

Malmierca MS, Blackstad TW, Osen KK. Computer-assisted 3-D reconstructions of Golgi-impregnated neurons in the cortical regions of the inferior colliculus of rat. Hear Res. 2011; 274(1–2):13–26. [PubMed: 20600744]

Malmierca MS, Hernandez O, Falconi A, Lopez-Poveda EA, Merchan M, Rees A. The commissure of the inferior colliculus shapes frequency response areas in rat: an in vivo study using reversible blockade with microinjection of kynurenic acid. Exp Brain Res. 2003; 153(4):522–529. [PubMed: 14508633]

Malmierca MS, Izquierdo MA, Cristaudo S, Hernandez O, Perez-Gonzalez D, Covey E, Oliver DL. A discontinuous tonotopic organization in the inferior colliculus of the rat. J Neurosci. 2008; 28(18): 4767–4776. [PubMed: 18448653]

Mugnaini, E.; Oertel, W. An atlas of the distribution of GABAergic neurons and terminals in the rat CNS as revealed by GAD immunohistochemistry. In: Bjorklund, A.; Hokfelt, T., editors. Handbook of chemical neuroanatomy. New York: Elsevier; 1985.

Nakamoto KT, Mellott JG, Killius J, Storey-Workley ME, Sowick CS, Schofield BR. Analysis of excitatory synapses in the guinea pig inferior colliculus: a study using electron microscopy and GABA immunocytochemistry. Neuroscience. 2013; 237:170–183. [PubMed: 23395860]

Oertel D, Bal R, Gardner SM, Smith PH, Joris PX. Detection of synchrony in the activity of auditory nerve fibers by octopus cells of the mammalian cochlear nucleus. Proc Natl Acad Sci U S A. 2000; 97(22):11773–11779. [PubMed: 11050208]

Oliver DL, Kuwada S, Yin TC, Haberly LB, Henkel CK. Dendritic and axonal morphology of HRP-injected neurons in the inferior colliculus of the cat. J Comp Neurol. 1991; 303(1):75–100. [PubMed: 2005240]

Oliver DL, Morest DK. The central nucleus of the inferior colliculus in the cat. J Comp Neurol. 1984; 222(2):237–264. [PubMed: 6699209]

Peruzzi D, Bartlett E, Smith PH, Oliver DL. A monosynaptic GABAergic input from the inferior colliculus to the medial geniculate body in rat. J Neurosci. 1997; 17(10):3766–3777. [PubMed: 9133396]

Saint Marie RL, Stanforth DA, Jubelier EM. Substrate for rapid feedforward inhibition of the auditory forebrain. Brain Res. 1997; 765(1):173–176. [PubMed: 9310410]

Saldana E, Merchan MA. Intrinsic and commissural connections of the rat inferior colliculus. J Comp Neurol. 1992; 319(3):417–437. [PubMed: 1376335]

Saldana, E.; Merchan, MA. Intrinsic and commissural connections of the inferior colliculus. In: Winer, JA.; Schreiner, CE., editors. The Inferior Colliculus. New York: Springer; 2005. p. 155-181.

Sivaramakrishnan S, Sanchez JT, Grimsley CA. High concentrations of divalent cations isolate monosynaptic inputs from local circuits in the auditory midbrain. Front Neural Circuits. 2013; 7:175. [PubMed: 24194701]

Smith PH. Anatomy and physiology of multipolar cells in the rat inferior collicular cortex using the in vitro brain slice technique. J Neurosci. 1992; 12(9):3700–3715. [PubMed: 1356146]

Venkataraman Y, Bartlett EL. Post-Natal Development of Synaptic Properties of the GABAergic Projection from Inferior Colliculus to Auditory Thalamus. J Neurophysiol. 2013; 109(12):2866–2882. [PubMed: 23536710]

Wallace MN, Shackleton TM, Palmer AR. Morphological and physiological characteristics of laminar cells in the central nucleus of the inferior colliculus. Front Neural Circuits. 2012; 6:55. [PubMed: 22933991]

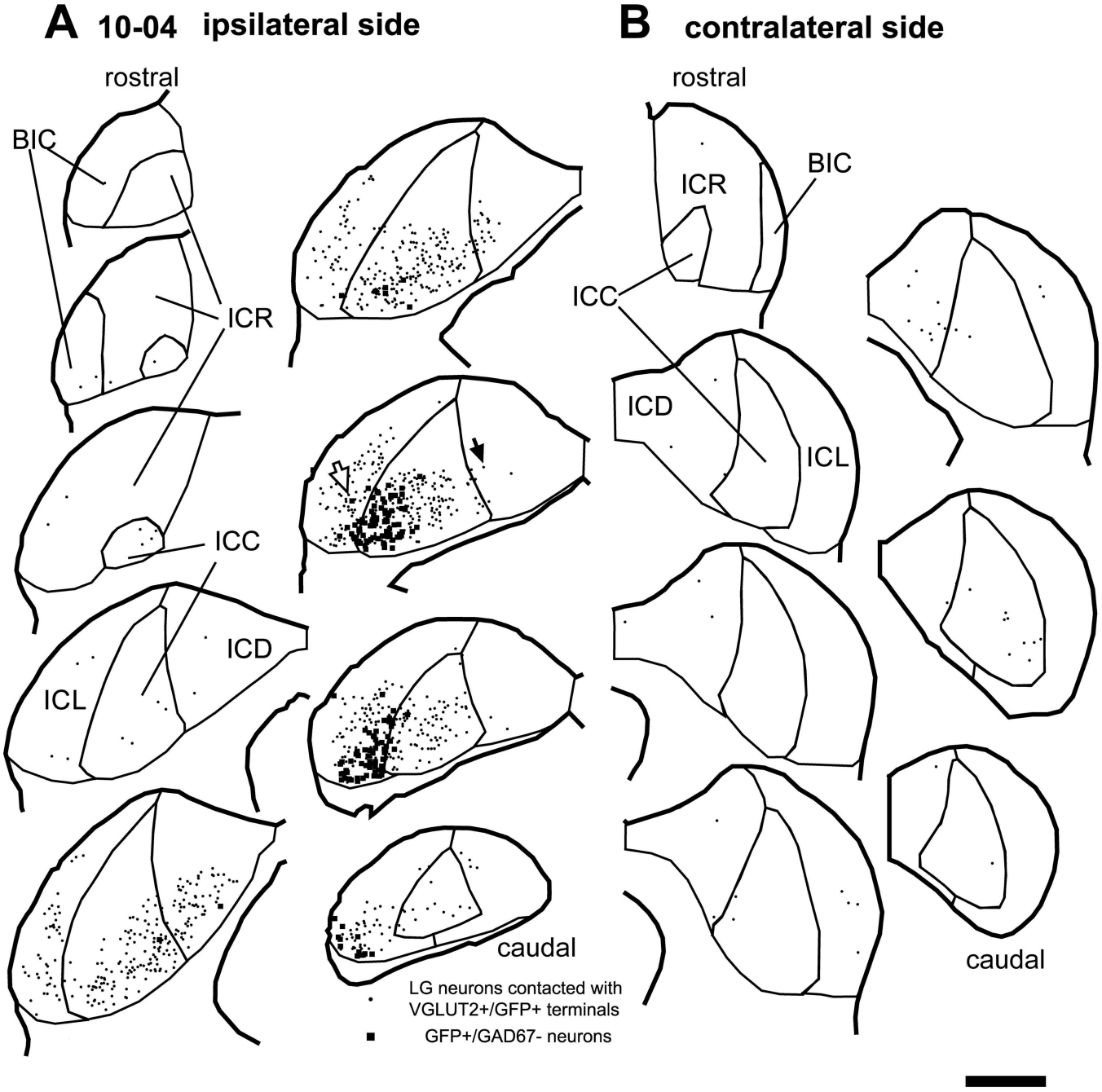

Figure 1.

Large GABAergic (LG) neurons (dots) that receive axosomatic contacts from GFP+/VGLUT2+ terminals after an injection of palGFP Sindbis virus. Case 10-04. Filled squares indicate non-GABAergic GFP+ neurons that are the source of GFP+/VGLUT2+ terminals. (**A**) On the ipsilateral side, LG cells receiving these inputs were relatively close to GFP+ neurons. (**B**) On the contralateral side, LG cells receiving contact with GFP+/VGLUT2+ terminals were primarily in the central nucleus (ICC) and dorsal cortex (ICD). Open and filled arrows indicate LG cells of Fig. 2A and 2C, respectively. Each trace is separated by a

distance of 240 μm. Abbreviations: BIC, brachium of the IC; ICR, rostral cortex; ICL, lateral cortex. Scale bar: 1 mm.

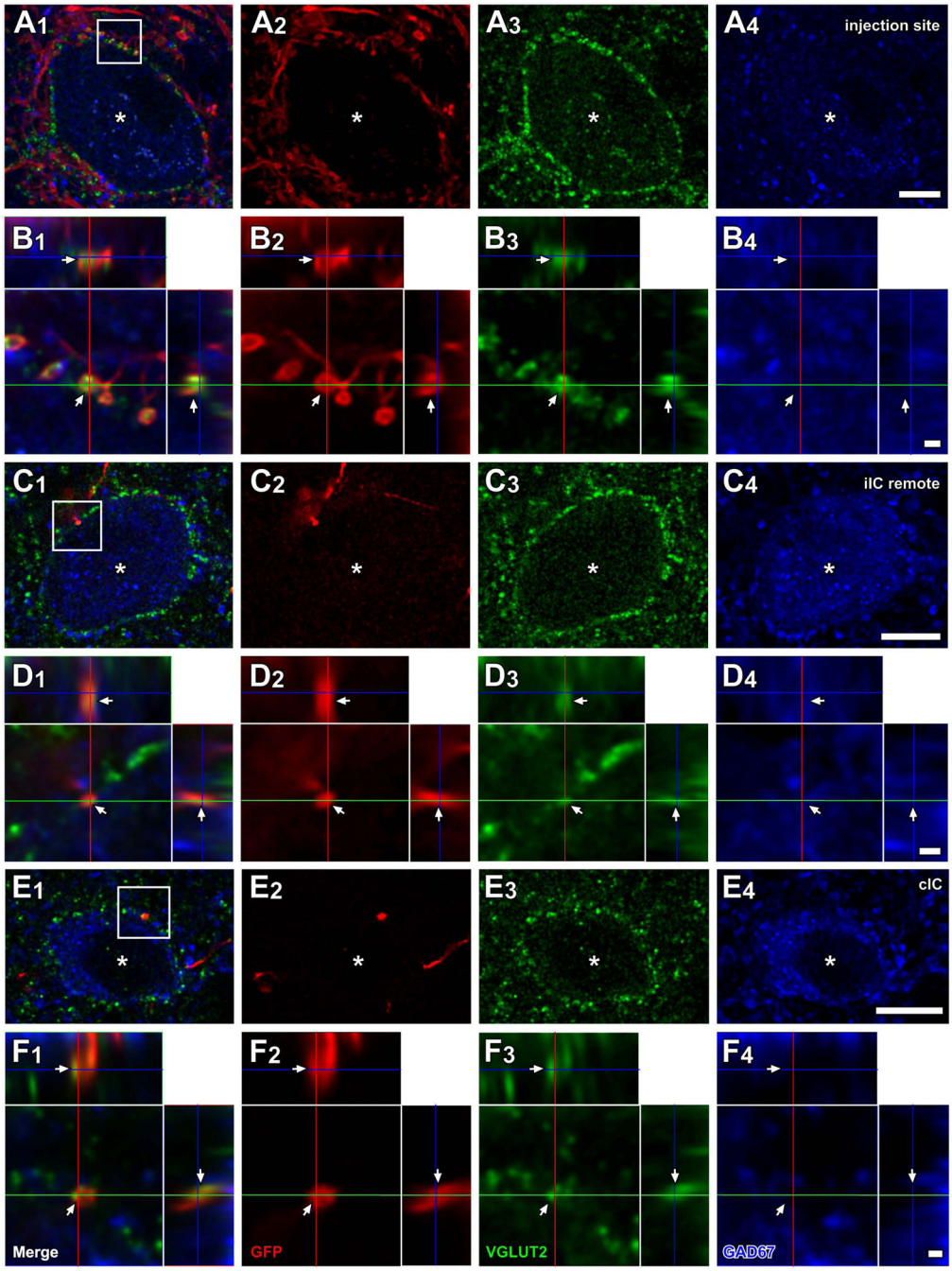

Figure 2.

LG cells receive excitatory inputs from local and commissural neurons. Images from case 10-04 are shown. (**A**) A LG cell located in the injection site (an open arrow in Fig. 1A). Numerous GFP+ (red) fibers were found around GAD67+ (blue) cell body (asterisks), and many of them made contact with the cell body. Most of these terminals were VGLUT2+ (green). (**B**) A higher-magnification image of a region of the cell body in **A$_1$** (box) with orthogonal views of the z-stack cut at 3 planes parallel to xy- (blue lines), yz- (a red line), and xz-planes (a green line). GFP+ terminals contained VGLUT2 (arrows). (**C**) A LG cell

(asterisks), located in the dorsal cortex of the IC, remote from the injection site (a filled arrow in Fig. 1A). Only a few GFP+ axons (one shown here) were found around the LG cell and made contact. (**D**) A higher-magnification image from $\mathbf{c_1}$ (box) with orthogonal views of the stack. Only a GFP+ terminal (arrows), which was also VGLUT2+, made contact on the LG cell. (**E**) A LG cell (asterisk) located in the ICD that received GFP+/VGLUT2+ axosomatic input. (**F**) A higher-magnification image from $\mathbf{E_1}$ (box) with orthogonal views of the stack. Scale bars: 10 μm (**A, C, E**), and 1 μm (**B, D, F**). Three-dimensional reconstructions of these GFP+ axons and LG cell bodies of **C** and **E** are shown in Fig. 8B and C.

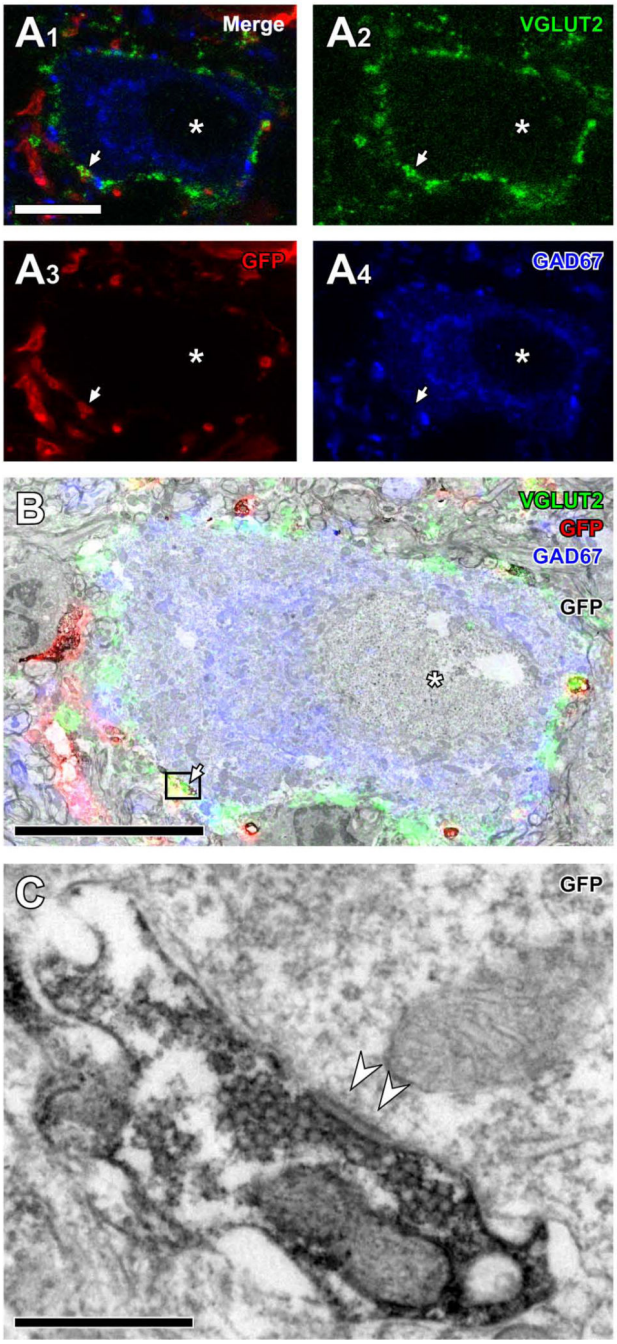

Figure 3.

Electron microscopic evidence of synapses made by GFP+/VGLUT2+ terminals on LG cell bodies. (**A**) Light microscopic images of a LG neuron, positive for GAD67 (blue, **A_4**), encircled by VGLUT2+ terminals (green, **A_1, A_3**) and receiving a contact from a terminal positive for both GFP (red, **A_1, A_3**) and VGLUT2. Asterisks indicate the nucleus of the LG neuron. (**B**) A superimposed image of **A_1** and an electron micrograph of the corresponding area. GFP immunoreactivity was visualized with a diaminobenzidine reaction. The arrow indicates the same terminal shown in **A**. The asterisk indicates the nucleus. (**C**) A high-

magnification electron micrograph of the terminal (box) in **B**. The terminal was immunopositive for GFP, contained numerous clear round vesicles, and made asymmetric axosomatic synapse (arrowheads) on the LG cell body. Scale bar: 10 μm (**A, B**) and 0.5 μm (**C**).

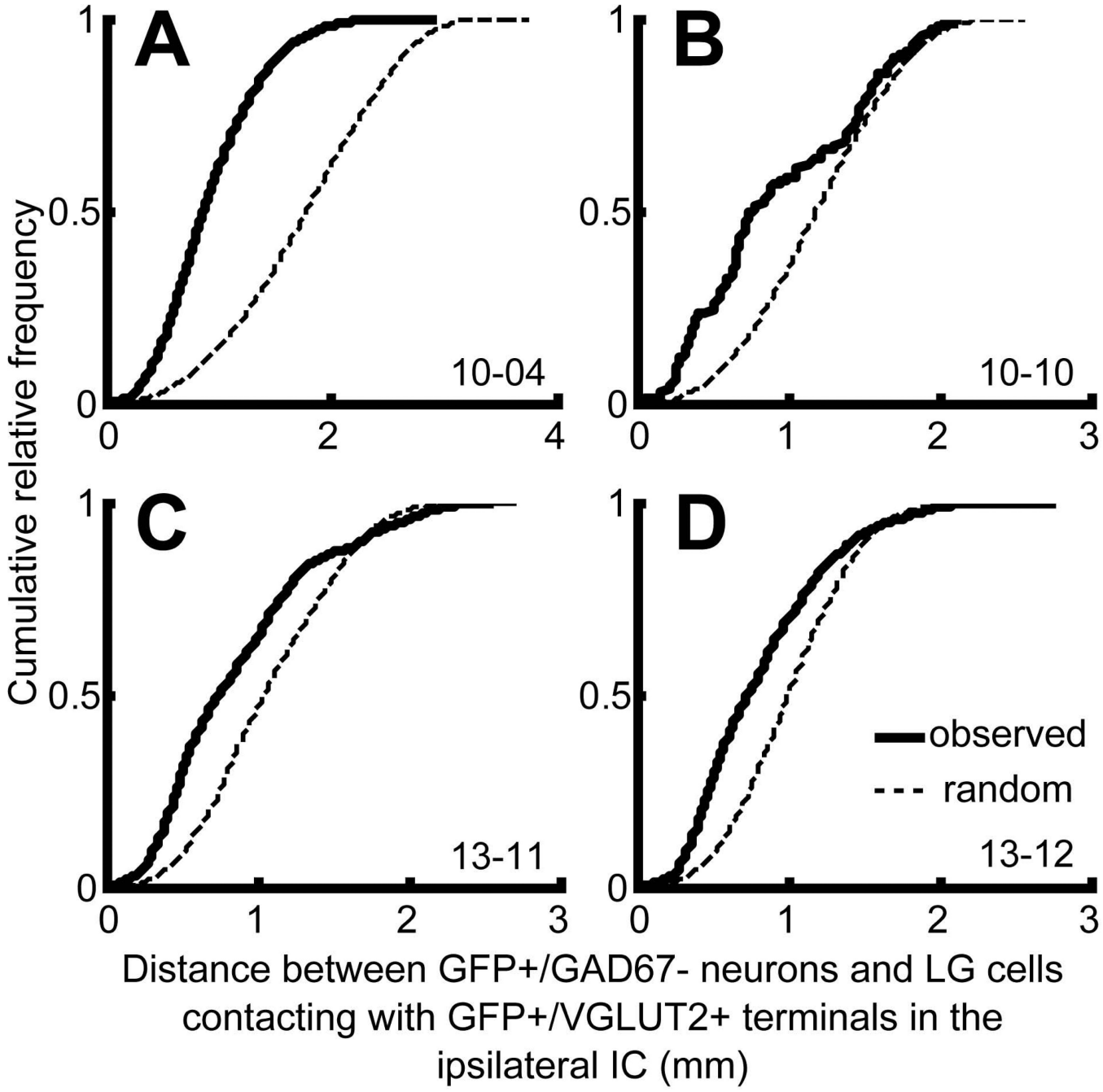

Figure 4.

Cumulative histograms of distance between ipsilateral, non-GABAergic GFP+ neurons and LG neurons receiving GFP+/VGLUT2+ terminals (thick lines). Dotted lines indicate cumulative histograms of distance between GFP+ neurons and randomly re-distributed LG cells. The observed distributions (thick lines) were significantly different from random distribution (dotted lines) ($P < 0.001$, Two-sample Kolmogolov-Smirnov test).

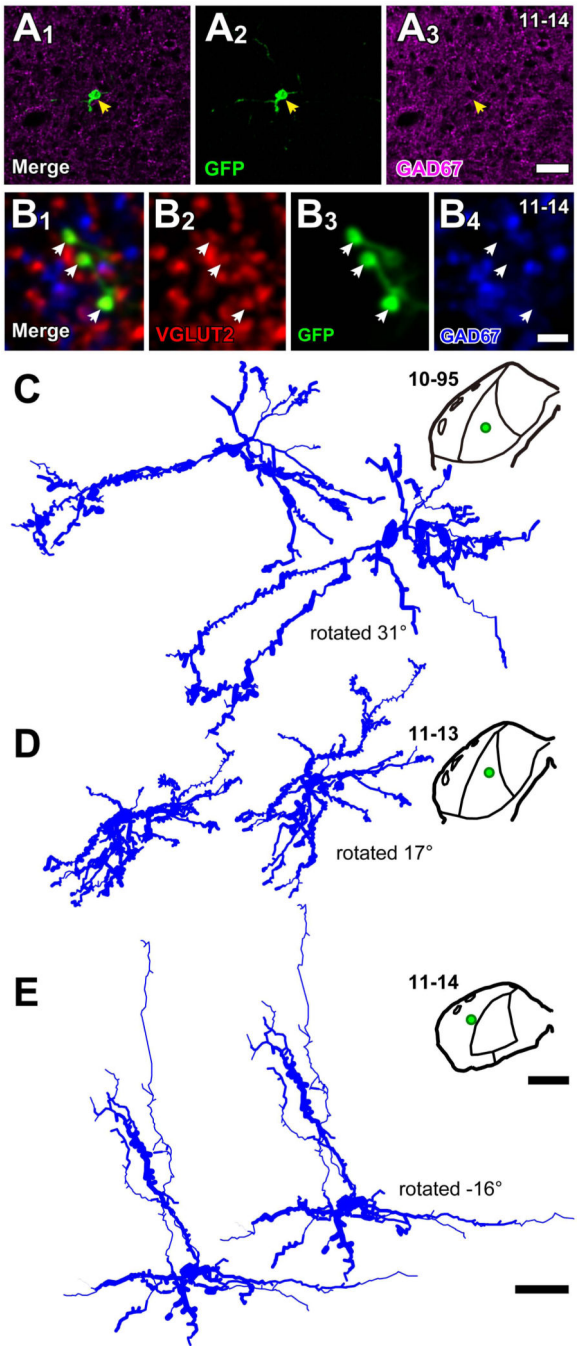

Figure 5.

Dendritic morphology of IC excitatory neurons revealed by labeling of single neurons (cases 10-95, 11-13, and 11-14). (**A**) A GFP+ (green) cell body (arrows) was negative for GAD67 (purple). Case 11-14. (**B**) Terminals of the GFP+ cell (green) were positive for VGLUT2 (red) and negative for GAD67 (blue). (**C–E**) Dendritic morphology and loci of GFP+ neurons. Two neurons with oriented dendrites in the ICC (cases 10-95 and 11-13) and a pyramidal-like neuron in the ICL layer 3 (case 11-14) were successfully reconstructed three-dimensionally. The reconstructions on left are in the original frontal plane of section, and

reconstructions on the right are rotated around medio-lateral axis. Green dots in the drawings of the IC indicate the loci of cell bodies. Note, the enhancement of immunoreaction by TSA system increased the thickness of the dendrites over that seen in fluorescent materials. Scale bars: 40 μm (**A**), 5 μm (**B**), 1 mm (whole IC drawings in **C–E**), and 50 μm (cell traces in **C–E**).

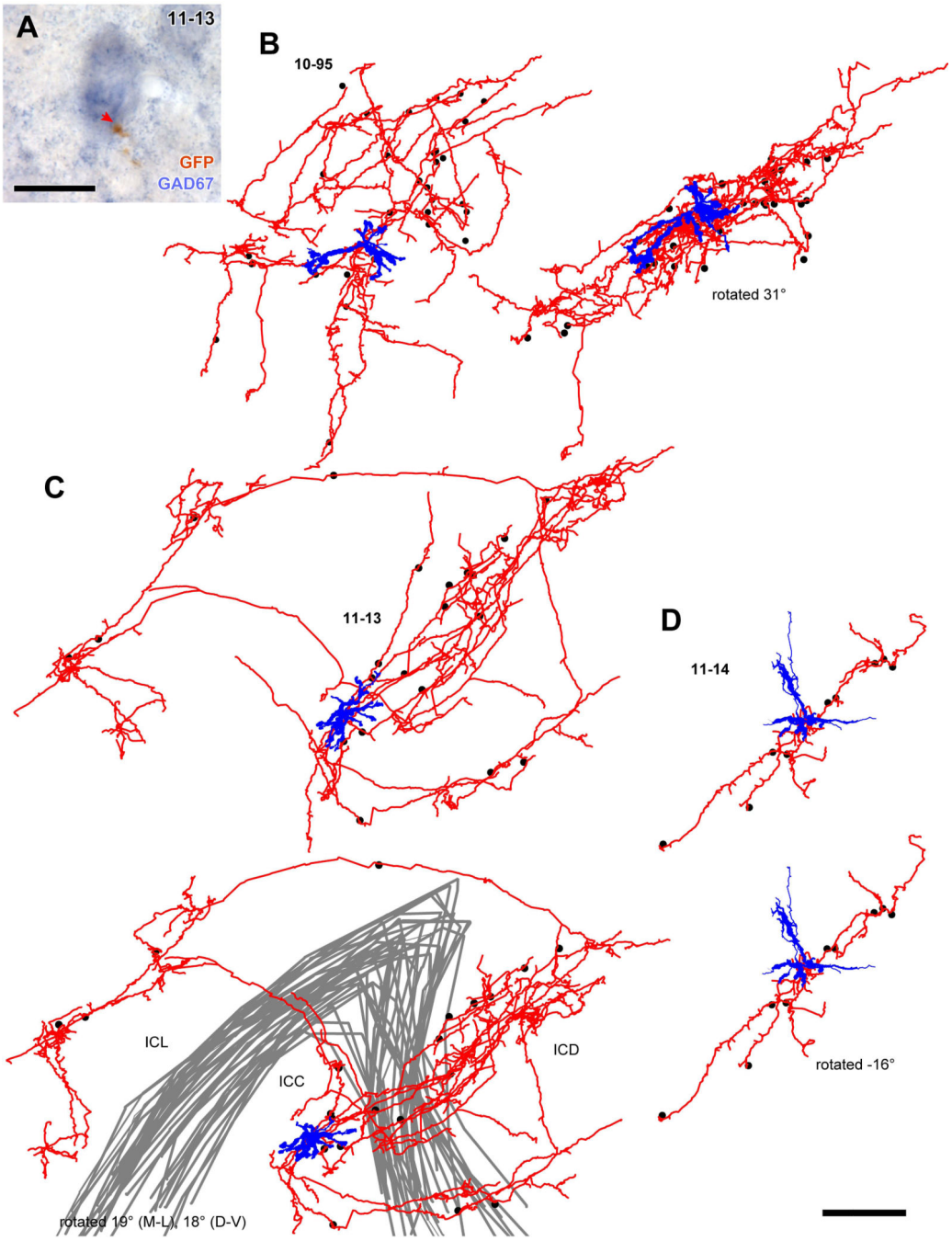

Figure 6.

Spatial distribution of GAD67+ cell bodies receiving axosomatic contact from axons of a single glutamatergic neuron. (**A**) An example of GAD67+ neuron (blue) that received axosomatic contact (a red arrow) with a GFP+ axon (brown). Case 11-13. (**B–D**) Reconstructed dendrites (blue) and axons (red) of GFP+ neurons shown in Fig. 5. Dots indicate cell bodies of GAD67+ neurons that receive one or more axosomatic contacts. In case 10-95 (**B**), the axonal plexus became flatter when the cell was rotated 31° around the medio-lateral axis. In case 11-14 (**D**) the cell had a poorly arborized axon, and the GAD67+

cells aligned well after a rotation of −16° around the medio-lateral axis. In the case 11-13 (**C**), axon collaterals made two planar plexuses in the ICC and ICD, and one plexus in the ICL. The GAD67+ cells receiving the axosomatic contacts were located in the dorsal and lateral cortices as well as in the ICC. Gray lines indicate the border of the ICC. Scale bars: 20 μm (**A**) and 250 μm (**B–D**).

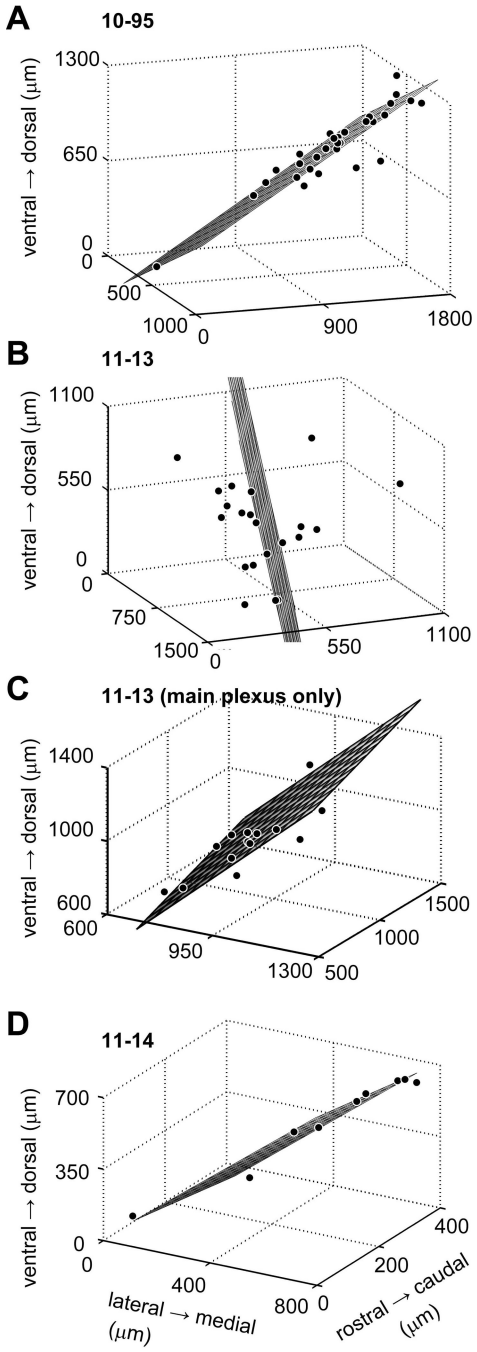

Figure 7.

Planar fits obtained by a principal component analysis (gray plane) and loci of GAD67+ cell bodies receiving axosomatic contact (dots). In the cases 10-95 (**A**) and 11-14 (**D**), GAD67+ cells were well-aligned to a plane. In case 11-13 (**B**) where there were two laminar plexuses, a planar fit for all GAD67+ cells was poor; however, there was a good planar fit for GAD67+ cells in the main axonal plexus (**C**).

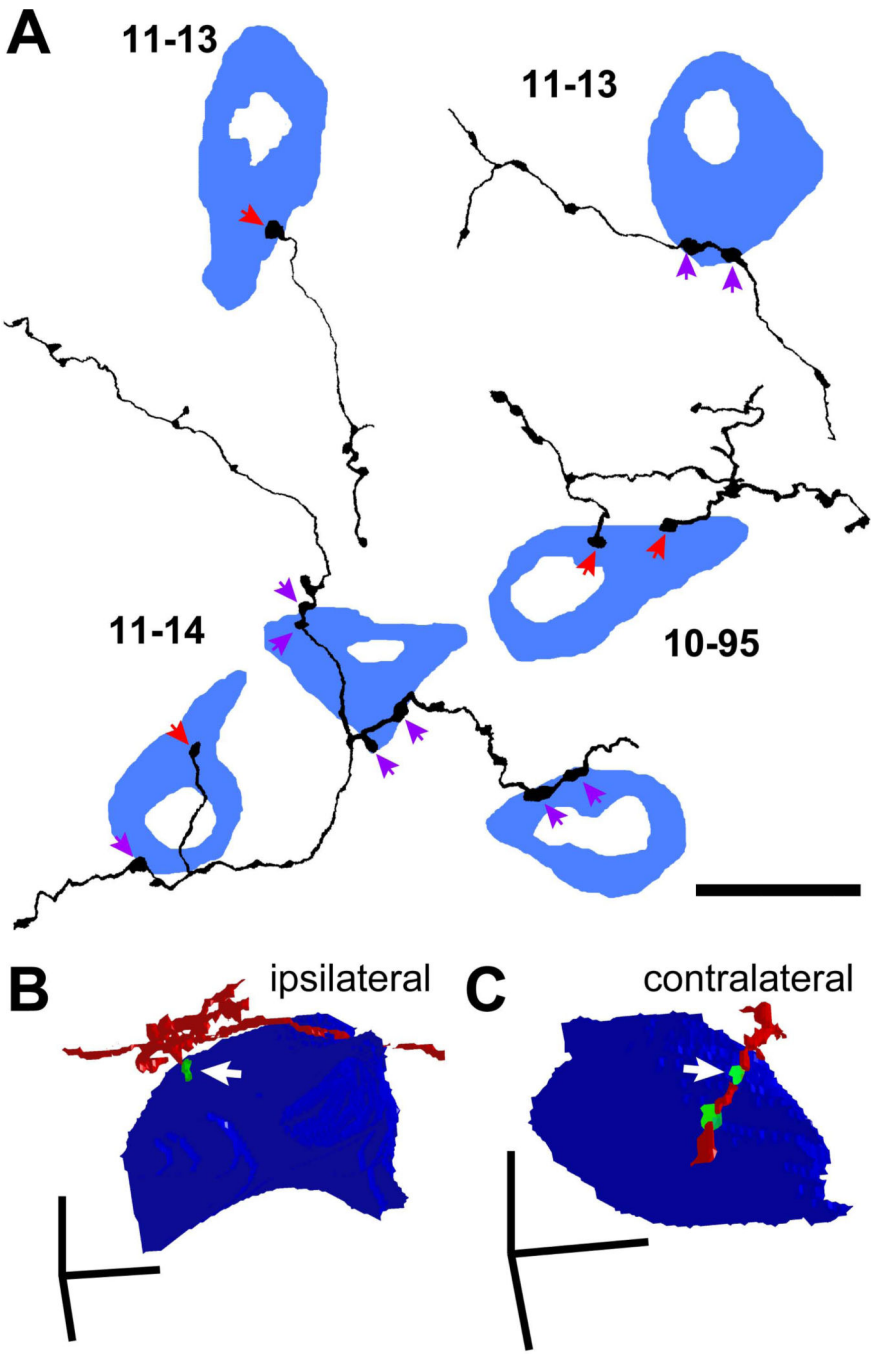

Figure 8.

Single axons made only a few axosomatic contacts on a single LG cell. (**A**) Termination patterns of GFP+ axons (black) on GAD67+ cells (blue) in the ipsilateral IC identified by bright-field double immunohistochemistry for GFP and GAD67. Some GABAergic cells were innervated by *en passant* varicosities (purple arrows) and the others were innervated by terminal boutons (red arrows). Note that a cell in the left-top is the same cell shown in Fig. 6A. (**B, C**) Three-dimensional reconstruction of GFP+ axons (red), GFP+/VGLUT2+ terminals (green), and LG neural cell bodies (blue) shown in Fig. 2C (ipsilateral) and **2E**

(contralateral). The axon in **B** made a terminal bouton on the LG cell body, while the axon in **C** made *en passant* contact. Arrows indicate the same axosomatic terminals shown in Fig. 2. Case 10-04. Scale bars: 20 μm (**A**) and 10 μm (**B, C**).

Table 1

Animals that received viral injections. BIC, brachium of the inferior colliculus (IC); ICC, central nucleus of the IC; ICD, dorsal cortex of the IC; ICL, lateral cortex of the IC; ICR, rostral cortex of the IC.

	Case #	Location of GFP+ cell bodies	Case #	Location of GFP+ cell bodies
large injection cases	09-14	ICR, ICD, ICL	10-44	ICC, ICL
	10-03	ICC, ICD, ICL	10-45	ICC, ICL
	10-04	ICC, ICD, ICL	10-46	ICC, ICL
	10-05	ICC, ICR, ICD	11-05	ICC, BIC, ICR, ICD, ICL
	10-10	ICC, ICR	11-10	ICC, ICL
	10-12	ICC	13-11	ICC, ICR
	10-39	ICC, ICL	13-12	ICC, ICL
single cell labeling cases	10-95	ICC		
	11-13	ICC		
	11-14	ICL		

Table 2

Table of Primary Antibodies Used

Antigen	Description of Immunogen	Source, Host Species, Cat. #, Clone or Lot#, RRID	Concentration Used
Glutamic acid decarboxylase 67 (GAD67)	Recombinant whole protein of rat GAD67.	Millipore, mouse monoclonal, Cat# MAB5406, RRID:AB_2278725.	1:1000.
Vesicular glutamate transporter 2 (VGLUT2)	KLH-conjugated, synthetic peptide corresponding to amino acids residues CWPNGWEKKEEFVQE SAQDAYSYKDRDDYS of rat VGLUT2 (aa. 554–582).	Professor Takeshi Kaneko (Kyoto University), guinea-pig and rabbit polyclonal.	0.5ug/ul
Green fluorescent protein (GFP)	recombinant whole protein of enhanced green fluorescent protein.	Professor Takeshi Kaneko (Kyoto University), rabbit polyclonal.	1ug/ul.

Table 3

The number of GFP+ neurons and LG neurons which received contact with terminals positive for both GFP and VGLUT2 in IC injection cases. ICR, rostral cortex of the IC; ICL, lateral cortex of the IC; ICD, dorsal cortex of the IC; ICC, central nucleus of the IC; BIC, brachium of the IC.

Case #	# GFP+ neurons										# LG neurons receiving contact with GFP+/VGLUT2+ terminals											
	GAD67-negative					GAD67-positive					Ipsilateral						contralateral					
	ICR	ICL	ICD	ICC	total	ICR	ICL	ICD	ICC	total (%)	BIC	ICR	ICL	ICD	ICC	total	BIC	ICR	ICL	ICD	ICC	total
10-04	0	69	1	91	161	0	4	0	6	10 (6.2%)	3	5	277	96	529	910	0	3	6	16	16	41
10-10	1	0	0	2	3	0	0	0	0	0 (0%)	1	3	5	0	30	39	0	0	0	0	0	0
13-11	37	0	0	2	39	6	0	0	0	6 (15.4%)	3	31	6	2	14	56	2	2	0	4	0	8
13-12	0	1	0	27	28	0	0	0	2	2 (7.1%)	3	21	57	11	104	196	0	4	6	1	0	11

Table 4

Summary of morphology of IC excitatory neurons

Case #	Location of the cell body	Mean diameter of the cell body (μm)	Total length of dendrites (μm)	Mean density of spines (μm^{-1})	Total length of axons (μm)	The number of contacted GAD+ neurons				Mean distance between the cell body and contacted GAD+ neurons (μm; mean ± SD)
						total	ICC	ICD	ICL	
10-95	ICC	12.8	3753	0.0234	40699	30	26	0	4	371 ± 150
11-13	ICC	14.7	3140	0.0465	44953	21	7	10	4	465 ± 235
11-14	ICL, layer 3	18.8	2821	0.0156	6372	9	0	0	9	229 ± 152

Table 5

Spatial distribution of GABAergic cells receiving contact from a single IC excitatory neuron.

Case #	SD of the 1st PC score (μm)	SD of the 2nd PC score (μm)	SD of the 3rd PC score (μm)	Rotation angle among M-L axis
10-95	423.8	260.7	69.7	31.1°
11-13	382.8	274.1	202.3	98.9°
11-13 (main plexus)	291.8	201.6	45.5	16.1°
11-14	312.2	41.3	27.7	−15.6°